Characterization of Hybrid Resin Systems Based on
Epoxy and Acrylate Functionalities

Ying Cai and Julie L. P. Jessop, Chemical & Biochemical Engineering, University of Iowa

Abstract:

Raman spectroscopy was used to study hybrid monomers containing epoxide functional groups undergoing cationic photopolymerization and acrylate functional groups undergoing free radical photopolymerization. The kinetics of the two mechanisms have been differentiated in real time. The effects of processing variables such as light intensity and photoinitiator systems were compared. Raman microscopy provided the conversion distribution of functional groups across the surface of the photopolymers.

Introduction

Hybrid systems, which contain two functional groups polymerized by independent reaction mechanisms, have arisen in recent years. For example, free radical and cationic photopolymerization chemistries have been combined to produce acrylate/epoxide (1,2) and acrylate/vinyl ether (3,4) hybrid polymers. This paper focuses on the study of epoxide/acrylate hybrid systems using Raman spectroscopy. Acrylates, which undergo free radical polymerization, exhibit high reaction rates and present a large selection of monomers and initiators, while epoxides, which undergo cationic ring opening photopolymerization, do not suffer from oxygen inhibition and exhibit low shrinkage. The potential control of the hybrid reaction process and the ability to tailor the resulting hybrid polymer structure promise less shrinkage, lower sensitivity to both oxygen and moisture, and desired properties, such as improved adhesion, hardness, and flexibility. These photopolymers are well-suited for coating materials, adhesives and dental restoratives (2,5,6). Although some hybrid systems have been developed, the reaction mechanisms have not been investigated in great detail. The deficiency of basic understanding hinders their application and tailored formulation for desired photopolymers.

Several analytical methods are available for *in-situ* polymerization investigation. Differential scanning calorimetry (DSC) has been adapted to photopolymerization systems to enable real-time kinetic study (7,8). However, DSC is not able to follow the conversion of two different functional groups individually since it measures the overall heat of reaction released by the system. Spectroscopic methods, such as real-time infrared (RTIR) (1,4) and Raman (9) spectroscopy, enable the real-time study of different functionalities in hybrid systems. Although mid-infrared (MIR) spectroscopy has been used for reaction kinetic studies, the requirements on sample size and preparation limit its application. Both near-infrared (NIR) and Raman spectroscopy are non-destructive techniques that allow analysis of multi-dimensional samples. Raman has been shown to be a valuable technique for both qualitative and quantitative analysis of all kinds of materials and systems (9,10,11). This paper demonstrates that Raman spectroscopy is able to differentiate the photopolymerization of epoxide rings and acrylate double bonds simultaneously in real time. A conversion distribution map of both functional groups across the surface of the hybrid polymer is also attainable by combining Raman spectroscopy with microscopy.

Experimental

Materials. The hybrid resins used in this study contain an acrylate double bond and an epoxide ring and were chosen to study chemical structural effects upon monomer reactivity. The photoinitiators used in this study were the α-cleavable free radical initiator DMPA and the cationic initiator DAI based on diaryliodonium salts.   All materials are listed in Table 1 and were used as received.

Table 1. Monomers and photoinitiators used in this research

Function	Chemical Name	Acronym/Source	Structure
Hybrid monomers	3,4-epoxy-cyclohexyl-methyl methacrylate	**METHB** (Daicel)	
	3,4-epoxy-cyclohexyl-methyl acrylate	**AETHB** (Daicel)	
	glycidyl methacrylate	**GMA** (Aldrich)	
Cationic photoinitiator	diaryliodonium hexafluoroantimonate	**DAI** (Sartomer)	$C_{12}H_{25}CHCH_2O-$ ... I^+ ... SbF_6^-, OH
Free radical photoinitiator	2,2-dimethoxy-2-phenylacetophenone	**DMPA** (Aldrich)	OCH_3, OCH_3

Methods.   A 785-nm NIR laser was used to induce the Raman scattering effect.   Spectra of monomers were collected using a Leica DMLP optical microscope attached to the HoloLab 5000R modular research Raman spectrograph (Kaiser Optical Systems, Inc).   The exposure time for spectra was 5 s.   An xyz stage with 0.1-µm step resolution enabled area mapping of the sample surface.   The step size for area mapping was 3 µm, and the exposure time was 30 s.   Samples were cured in a DSC aluminum pan using a 200-W Hg(Xe) lamp (Oriel).

Real-time data were collected using the Mark II holographic fiber-coupled stretch probehead (Kaiser Optical Systems, Inc.) attached to the HoloLab 5000R modular research Raman spectrograph. Samples were cured isothermally in 1-mm ID quartz capillary tubes using an Acticure® Ultraviolet/Visible Spot Cure System (EFOS) (shown in Figure 1).   The exposure time for spectra was 500 ms.
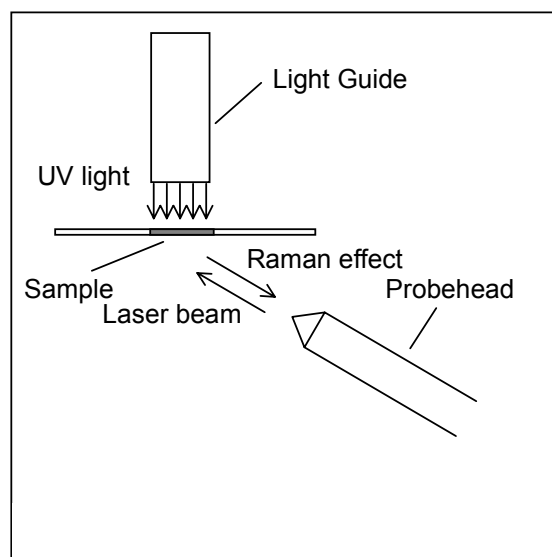
Results and Discussion

Raman spectroscopy allows quantitative identification of functional groups and qualitative determination of their concentration.   In polymerizations, the disappearance of certain Raman bands is proportional to the monomer conversion.   According to Equation 1 (12), by ratioing the peak area of a reactive band (A_{rxn}), which is associated with the reactive functionality, to an internal reference band (A_{ref}), which is associated with a portion of the monomer molecule that does not enter into the reaction, the conversion of the reactive functional group can be calculated.   The rate of reaction can then be obtained by differentiating the resulting conversion profile.

$$\alpha = 1 - \frac{A_{rxn}(t) \big/ A_{ref}(t)}{A_{rxn}(0) \big/ A_{ref}(0)} \qquad (1)$$

Raman Spectra of Hybrid Monomers. The spectra of three hybrid monomers (GMA, METHB, and AETHB) were obtained using Raman microscopy with a 10X objective (see Figure 2 below).   By comparing spectra of the monomers and their respective polymer, characteristic Raman bands associated with reactive and non-reactive functionalities were identified (see Table 2 below) (13,14,15).   For both acrylate (AETHB) and methacrylate (METHB and GMA) monomers, reactive bands for the C=C bond are located at 1640 cm^{-1} and 1410 cm^{-1}.   Raman bands representing the epoxide ring can exist in a wide range. For the cycloaliphatic epoxides (METHB and AETHB), there is a strong peak at 790 cm^{-1}; for the aliphatic epoxide (GMA), this reactive band is at 750 cm^{-1}.   A reference band at 605 cm^{-1} was selected for the methacrylates (GMA and METHB); however, the reference band for AETHB is still under investigation.   Ratios of these bands were used to calculate polymer conversion and composition.

Real-time Raman Spectroscopy of METHB.   Isothermal photopolymerizations of METHB were carried out at 50°C with different initiator systems.   Figure 3 (below) shows the change in the Raman spectrum of METHB as the free radical photopolymerization proceeds. The reactive band at 1640 cm^{-1}, which represents the concentration of the C=C bond, decreases upon irradiation; whereas the reference band at 605 cm^{-1}, which represents the concentration of the COO bond, remains constant throughout the reaction.   Since the reference band does not change during the reaction, the double bond conversion was then calculated by modifiying Equation 1 to include only the peak area of the reactive band (A_{rxn}):

$$\alpha = 1 - \frac{A_{rxn}(t)}{A_{rxn}(0)} \qquad (2)$$
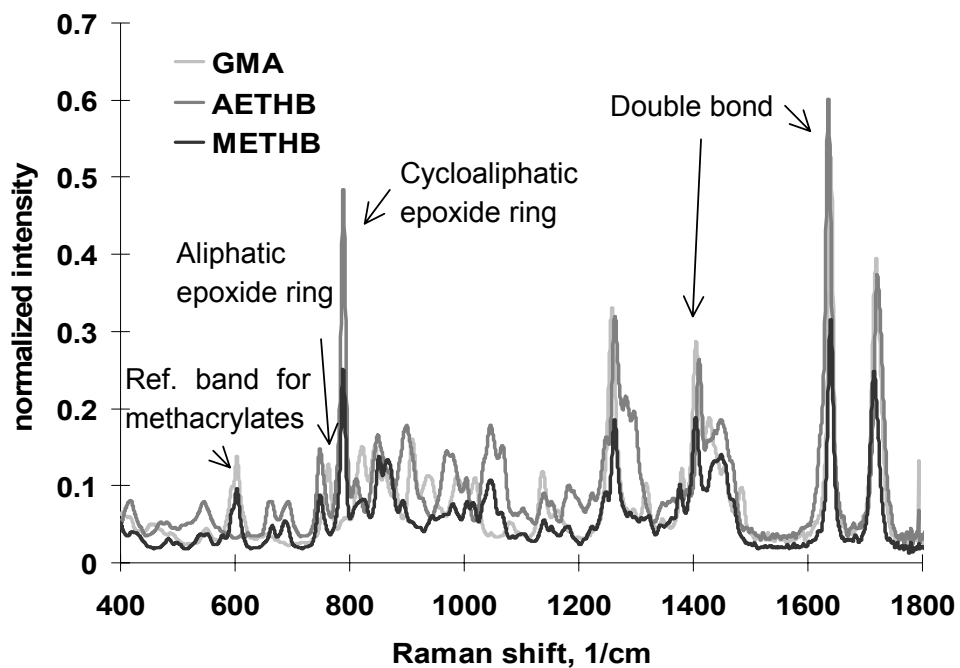
Figure 2. Raman spectra of hybrid monomers: GMA, AETHB and METHB

Table 2. Characteristic Raman bands for the hybrid monomers

	Acrylic double bond	Epoxide ring	Reference peak
GMA	1640 cm^{-1}, 1410 cm^{-1}	750 cm^{-1}	605 cm^{-1}
AETHB	1640 cm^{-1}, 1410 cm^{-1}	790 cm^{-1}	—
METHB	1640 cm^{-1}, 1410 cm^{-1}	790 cm^{-1}	605 cm^{-1}
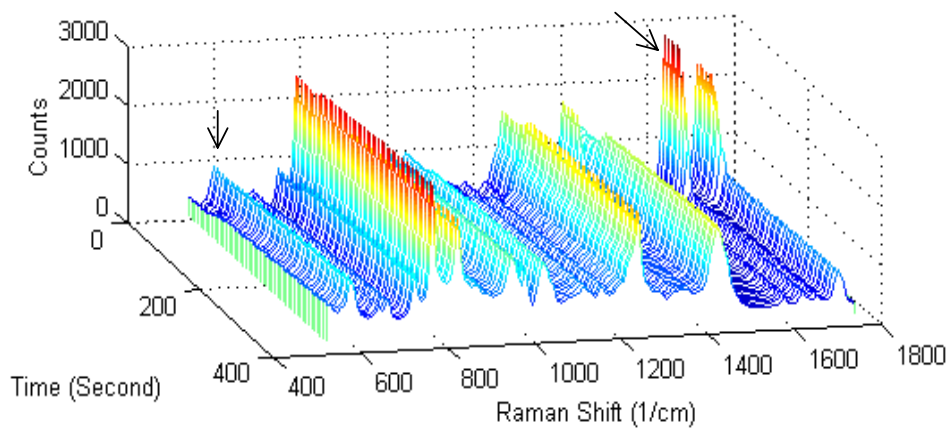
Figure 3. 3-D picture of real-time Raman reaction monitoring of METHB with 2wt% DMPA at 50ºC and light intensity of 100 mW/cm^2.

Two important processing variables, namely initiator concentration and light intensity, were studied by using this real-time Raman technique. The conversion profiles of the acrylate double bond and the epoxide ring of METHB with different concentrations of free radical photoinitiator DMPA and/or cationic photoinitiator DAI are presented in Figures 4 and 5. When only the free radical photoinitiator is used in the system (Figure 4, left), the conversion of acrylate and the rate of polymerization increases as the initiator concentration is increased. When only the cationic photoinitiator is used in the system (Figure 4, right), the time to ultimate conversion decreases and the rate of polymerization increases as the initiator concentration is increased. However, when both photoinitiators are used in the system (Figure 5), the conversion of each functional group is less than in the systems with a single photoinitiator at the same concentration. This is due in part to the cross-linked network that is being formed in the system as both the acrylate and epoxide groups react simultaneously.
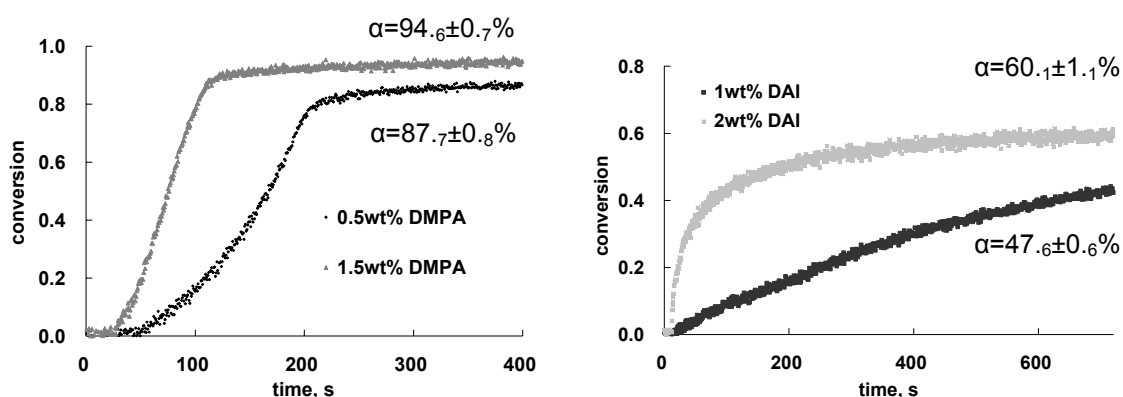
Figure 4. Conversion profiles of METHB with only the free radical initiator DMPA (left) and only the cationic initiator DAI (right) at 50°C and light intensity of 100 mW/cm^2.
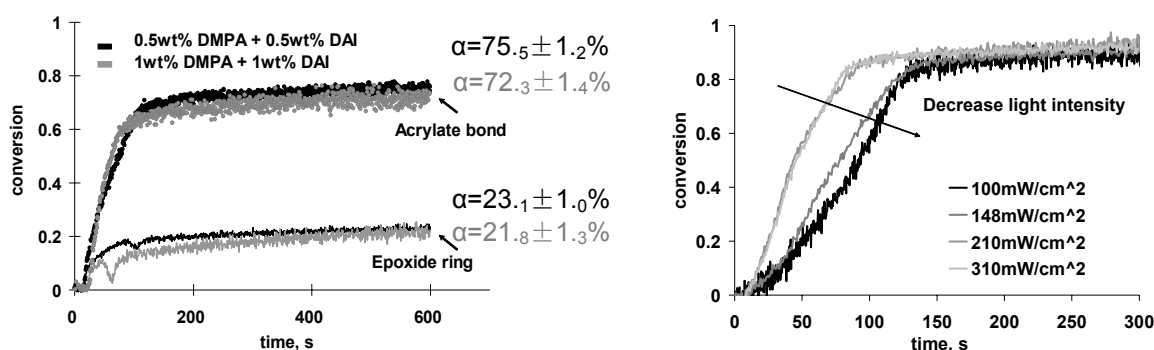
Figure 5. Conversion profiles of METHB with both DMPA and DAI at 50°C and light intensity of 100 mW/cm^2.

Figure 6. Conversion profiles of METHB with 1wt% DMPA at 50°C and various light intensities.
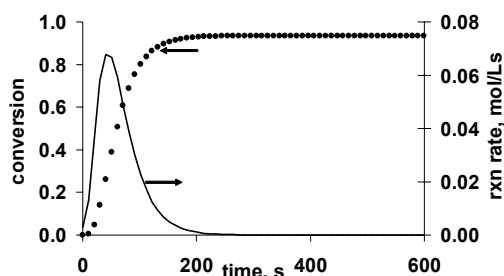
The conversion profiles of the acrylate double bond in METHB with different light intensities are presented in Figure 6 (above). In these studies, increasing the light intensity increases the rate of polymerization; however, a limiting conversion of 90% is seen in this free radical photopolymerization system regardless of the light intensity. These intensity data will be used to optimize process conditions, as well as to validate kinetic models, in future studies.

The reaction rate can then be calculated from the conversion profile. Figure 7 shows an example of METHB with 2wt% DMPA (conversion profile shown in Figure 4, left). The conversion data were smoothed using a five-point fast Fourier transform (FFT) and then fitted with a sigmoidal model in Origin (Microcal). The fitted data were then differentiated to generate the rate of polymerization as a function of time. Future studies will compare the reaction rates of the acrylate and epoxide functionalities in the three hybrid resins.

Conversion Distribution of Hybrid Polymers. The conversion of acrylate double bonds and epoxide rings across the surface of the hybrid polymer METHB cured using 0.5wt% DMPA and 0.5wt% DAI was determined by Raman microscopy with a 50X long-working distance objective. Figure 8 shows the resulting 3-D maps for the intensity of the acrylate C=C Raman band (left) and epoxide ring Raman band (right). Higher relative intensities of the respective reactive bands indicate lower functional group conversion. The conversion of both functionalities is shown in Figure 9 (below) for the line at y = 15 µm. The conversions are not consistent across the surface, ranging from 78.6% to 86.3% for double bond and 17.0% to 28.3% for epoxide ring. However, high acrylate conversion in one area is not correlated with low epoxide conversion in that same area (and *vice versa*).
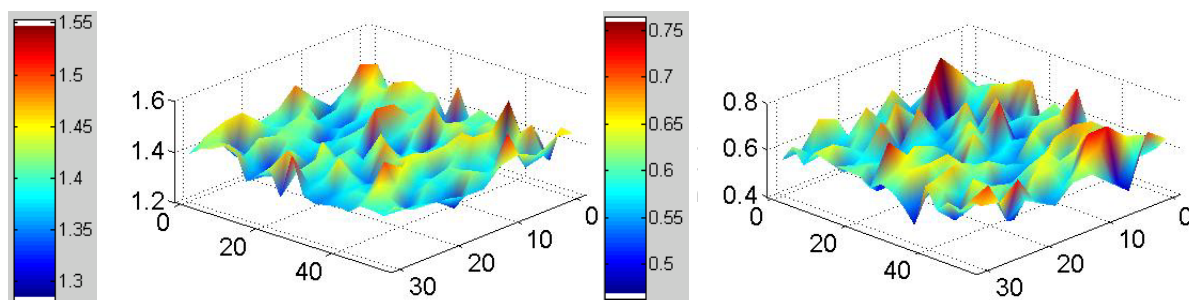
Figure 8. The relative intensity peak area ratio of the acrylate C=C band at 1640 cm^{-1} (left) and the epoxide ring band at 790 cm^{-1} (right) with the reference band at 605 cm^{-1} across the selected area of an METHB hybrid polymer surface. The sample was cured using 0.5wt% DMPA and 0.5wt% DAI at T = 50°C with light intensity = 100 mW/cm^2.
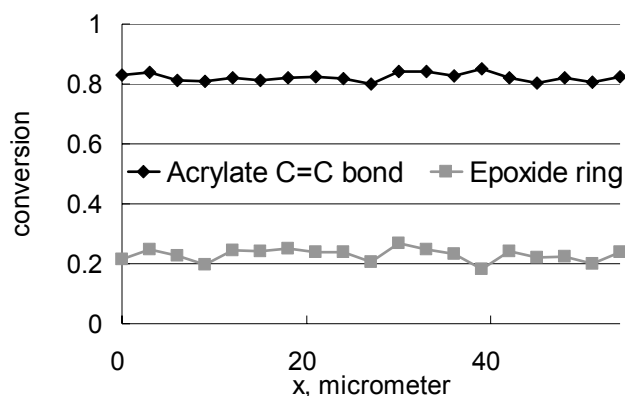
Figure 9. The conversion of acrylate double bond and epoxide ring at the y = 15 μm line of the Raman area map investigated in Figure 8.

Conclusions

Raman spectroscopy is effective for both kinetic and chemical composition studies of hybrid photopolymer systems.   The Raman probehead is capable of following the changes of the different functional groups simultaneously with high time resolution. The Raman microscope enables the quantitative and qualitative analysis of chemical characteristics of the resulting photopolymers.   Photoinitiator concentration and light intensity effects upon conversion were briefly studied and will require further investigation.   Future kinetic study will use these Raman techniques to compare the chemical structural effect upon monomer reactivity and to determine the effects of other processing variables, such as temperature and atmospheric inhibitors.   These results will be use to optimize systematically hybrid polymers for specific applications.

Acknowledgements

References

1. C. Decker, T. Nguyen Thi Viet, D. Decker, E. Weber-Koehl, *Polymer* 42, 5531 (2001).
2. J. D. Oxman, D. W. Jacobs, M. C. Trom, *Polymeric Materials: Science & Engineering*, 88, 239 (2003).
3. S. K. Rajaraman, W. A. Mowers, J. V. Crivello, *J. Polym. Sci., Part A: Polym. Chem.*, 37, 4007 (1999).
4. Y. Lin and J. W. Stansbury, *Polymer*, 44, 4781, (2003).
5. C. Decker, *Macromol. Rapid Commun.,* 23, 1067 (2002).
6. Y. Lin and J. W. Stansbury, *Polymer Preprints*, 43, 354, (2002).
7. B. Sandner, N. Kotzian, J. Tubke, S. Wartewig, D. Lange, *Macromol. Chem. Phys.,* 198, 2715 (1997).

8. I. V. Khudyakow, J. C. Legg, M. B. Purvis, B. J. Overton, *Ind. Eng. Chem. Res.,* 38, 3353 (1999).
9. E. W. Nelson and A. B. Scranton, *J. Polym. Sci., Polym. Chem. Ed.,* 34, 403 (1996).
10. J. C. Merino, M. del R. Fernandez, and J. M. Pastor, *Micromol. Symp.*, 168, 55 (2001).
11. H. G. M. Edwards, A. F. Johnson, I. R. Lewis, *J. Raman Spectrosc.* 24, 475 (1993).
12. M. Younes, S. Wartewig, D. Lellinger, B. Strehmel, V. Strehmel, *Polymer*, 35, 5269 (1994).
13. D. Lin-Vien, N. B. Colthup, W. G. Fateley, J. G. Grasselli, *The Handbook of Infrared and Raman Characteristic Frequencies of Organic Molecules*, Academic Press, San Diego, 1991.
14. N. B. Colthup, L. H. Daly, S. E. Wiberley, *Introduction to Infrared and Raman Spectroscopy*, 3rd Ed., Academic Press, San Diego, 1990.
15. R. A. Nyquist, *Interpreting Infrared, Raman, and Nuclear Magnetic Resonance Spectra, Vol. 1 & 2*, Academic Press, San Diego, 2001.